

# Drag forces on inclusions in classical fields with dissipative dynamics

V. Démery and D.S. Dean<sup>a</sup>

Laboratoire de Physique Théorique, IRSAMC, Université de Toulouse UPS and CNRS, 31062 Toulouse Cedex 4, France

Received 1 April 2010

© EDP Sciences / Società Italiana di Fisica / Springer-Verlag 2010

**Abstract.** We study the drag force on uniformly moving inclusions which interact linearly with dynamical free field theories commonly used to study soft condensed matter systems. Drag forces are shown to be nonlinear functions of the inclusion velocity and depend strongly on the field dynamics. The general results obtained can be used to explain drag forces in Ising systems and also predict the existence of drag forces on proteins in membranes due to couplings to various physical parameters of the membrane such as composition, phase and height fluctuations.

## 1 Introduction

Quantum field theory explains how particles can interact at a distance via their coupling to a quantum field [1]. However, interaction at a distance also occurs in classical systems where particles or inclusions are coupled to classical thermal fields. For instance inclusions embedded in lipid membranes can interact due to their coupling with the membrane height fluctuations [2] or with the local lipid composition [3]. As well as effective interactions between inclusions, coupling to a classical field can also show up in the transport properties of inclusions in these fields, notably via drag forces which can be generated and act upon uniformly moving inclusions. The knowledge of drag forces is important as they can be used to estimate effective transport parameters, for example diffusion constants by using the Stokes-Einstein relation. Drag forces have been studied in a wide variety of systems, for instance on line defects moving through liquid crystals [4, 5] and on dislocations in layered structures [6] and quasicrystals [7]. As well as being present for inclusions in a field, drag forces are also experienced by objects outside but interacting with the field, for instance magnetic force microscope tips interacting with magnetic substrates [8, 9]. In a recent letter [10] we analyzed the drag on an inclusion which interacts with the fluctuating field, for example a magnetic field at a point which moves through an Ising ferromagnet. Our analysis was restricted to free scalar fields undergoing a general class of overdamped dissipative dynamics. A number of remarkable features were found for the drag in this class of problems: i) the average drag force  $\langle f \rangle$  is a nonlinear function of the velocity, in general it is linear for small  $v$  and is characterized by

a friction coefficient  $\lambda = -\lim_{v \rightarrow 0} \langle f \rangle / v$ . ii) In systems where the free-field theory is critical (has a diverging correlation length) this friction coefficient can diverge and is regularized by the system size. iii) At large velocities the average force decays to zero as  $\langle f \rangle \sim 1/v$ . It was also found that numerical simulations for the drag in the Ising model could be well fitted using results for free fields (corresponding to the Gaussian approximation for the field theory of the ferromagnet).

In this paper we will give an extended account of the results and derivations of [10]. In addition we will show how the divergence of the friction coefficient  $\lambda$  can be regularized by looking at the system at a finite time after the inclusion starts to move, rather than in its steady state, and show that it diverges as a power law in time. The fluctuations of the force about its mean value are also analyzed and we show that the zero-velocity fluctuations of the force are related to the linear friction coefficient via a fluctuation-dissipation type relation. We also pay particular attention to computations of drag coefficients in two-dimensional systems. The reason for this is that there has been much recent interest in the diffusion constant for proteins in lipid membranes. The first theoretical computation of the diffusion constant of a protein in a lipid membrane treats the protein as a solid cylinder in a two-dimensional incompressible fluid layer hydrodynamically coupled to the surrounding bulk fluid [11]. The drag force on the fluid can be computed and one finds that, via the Stokes-Einstein relation, the diffusion constant has a weak logarithmic dependence on the cylinder radius  $a$ . Here we explore the possibility that drag may be generated by coupling to one of the several possible physical fields associated with the membrane, for instance height fluctuations, thickness fluctuations, composition fluctuations, local phase fluctuations. As mentioned above, in [10]

<sup>a</sup> e-mail: dean@irsamc.ups-tlse.fr

it was noted that drag forces in Ising models, which are clearly interacting models, could be well fitted by computations based on free-field theories. In general we have no explanation for this, but in this paper we have analyzed the drag forces in the one-dimensional Ising model with Glauber dynamics with a (weak) point-like magnetic field moving at constant velocity. We find an exact expression for  $\langle f \rangle$  which turns out to have the limiting form of model A dynamics for a free Gaussian theory in the continuum limit where the correlation length is large.

## 2 The free-field model

### 2.1 Model definition

In this section we will analyze the drag force exerted on an inclusion moving at constant velocity  $v$  which is linearly coupled to a Gaussian or free field. We denote by  $\phi(\mathbf{r})$  a scalar field on a  $d$ -dimensional space. We write the coordinates of the system as  $\mathbf{r} = (\mathbf{x}, z)$ , where the motion of the inclusion is in the  $z$ -direction. The Hamiltonian for the system is given by

$$H = \frac{1}{2} \int d\mathbf{r} \phi(\mathbf{r}) \Delta \phi(\mathbf{r}) - hK\phi(\mathbf{Q}(t)), \quad (1)$$

where  $\mathbf{Q}(t) = (\mathbf{0}, vt)$  is the position of the inclusion at time  $t$ ,  $\Delta$  is a positive self-adjoint operator and  $K$  a linear operator. The instantaneous force on the inclusion in the direction  $z$  is given by

$$f = h \frac{\partial}{\partial z} K\phi|_{\mathbf{r}=\mathbf{Q}(t)}, \quad (2)$$

*i.e.* it is simply the partial derivative of the total energy with respect to the movement of the inclusion in the direction  $z$ , with the field values held constant. The energetic formulation of the way in which the inclusion interacts with the field thus has the clear advantage, with respect to imposing boundary conditions, of giving an unambiguous way of computing the instantaneous force. This energetic approach was recently employed to compute the thermal Casimir force in a variety of field theories with dissipative dynamics of the type employed here [12].

Note that in the above we have used the operator notation

$$\Delta v(\mathbf{r}) = \int d\mathbf{r}' \Delta(\mathbf{r} - \mathbf{r}') v(\mathbf{r}'). \quad (3)$$

We will consider a general over-damped dissipative dynamics for the field  $\phi$  which can be written in the general form

$$\frac{\partial \phi(\mathbf{r})}{\partial t} = -R \frac{\delta H}{\delta \phi(\mathbf{r})} + \eta(\mathbf{r}, t), \quad (4)$$

where  $R$  is a positive self-adjoint dynamical operator and the noise is Gaussian, white in time, with correlation function

$$\langle \eta(\mathbf{r}, t) \eta(\mathbf{r}', t') \rangle = 2T \delta(t - t') R(\mathbf{r} - \mathbf{r}'). \quad (5)$$

This choice of the correlation function obeys the fluctuation dissipation relation which ensures that the equilibrium measure for the field is the Gibbs-Boltzmann one.

### 2.2 Specific examples and applications of the free field model

Before carrying out the general calculation we will give some examples of the sorts of field theories, interactions and dynamics that one can analyze with the formalism that follows. We start with various choices of the operator  $\Delta$ :

$$\Delta(\mathbf{r}) = (-\nabla^2 + m^2)\delta(\mathbf{r}), \quad (6)$$

$$\Delta(\mathbf{r}) = (\kappa \nabla^4 - \sigma \nabla^2)\delta(\mathbf{r}). \quad (7)$$

Equation (6) corresponds to the Gaussian approximation for the Hamiltonian of a ferromagnet in the Landau theory, as such the field  $\phi$  can be the local magnetization, the local composition of a binary fluid or another local order parameter. The form of eq. (7) comes from the Helfrich Hamiltonian for a lipid bilayer [13], where  $\phi$  represents the height fluctuations of the membrane about its average height. The term  $\kappa$  is the bending rigidity and the term  $\sigma$  is the surface tension. Still at the static level, there are a number of choices of the coupling of the inclusion to the field  $\phi$

$$K(\mathbf{r}) = \delta(\mathbf{r}), \quad (8)$$

$$K(\mathbf{r}) = \mathbf{d} \cdot \nabla \delta(\mathbf{r}), \quad (9)$$

$$K(\mathbf{r}) = \nabla^2 \delta(\mathbf{r}). \quad (10)$$

The coupling (8) is just a localized magnetic field, that in eq. (9) is a dipole (two fields of opposite sign close to each other) and eq. (10) arises in lipid membrane physics and represents a coupling to the membrane curvature, tending to induce the membrane to curve upwards or inwards. This sort of coupling arises for proteins whose structures are different in the upper and lower leaflets of the membrane bilayer and thus cause the membrane to become locally curved. For the dynamics there are a number of basic models that one can consider [14],

$$R(\mathbf{r}) = \delta(\mathbf{r}), \quad (11)$$

$$R(\mathbf{r}) = -\nabla^2 \delta(\mathbf{r}), \quad (12)$$

$$R(\mathbf{r}) = \frac{1}{(2\pi)^2} \int d\mathbf{k} \frac{\exp(i\mathbf{k} \cdot \mathbf{r})}{4\eta|\mathbf{k}|}. \quad (13)$$

The dynamical operator of eq. (11) corresponds to the simplest form of dissipative dynamics one can write down for a system whose total order parameter  $\bar{\phi} = \frac{1}{V} \int_V d\mathbf{r} \phi(\mathbf{r})$  is not conserved (also referred to as model A dynamics). This could apply to cases such as spin systems where  $\phi$  represents the local magnetization, or the local phase ordering parameter in lipid systems (solid, gel, liquid). The operator in eq. (12) corresponds to the simplest dynamics where the total order parameter is conserved, this should be the case for systems where  $\phi$  represents the local chemical composition and where the total number of each type of particle is conserved (model B dynamics). The operator of eq. (13) is the Oseen hydrodynamic kernel for membrane sheets, the field describes the height fluctuations of lipid membranes driven by a surrounding fluid of viscosity  $\eta$ . In eq. (13) the Oseen hydrodynamic kernel is defined via its (two-dimensional) Fourier transform.

### 2.3 General analysis of drag forces

With the explicit choice of the Hamiltonian in eq. (1), the equation of motion of the field is

$$\frac{\partial \phi(\mathbf{r})}{\partial t} = -R\Delta\phi(\mathbf{r}) + hRK^\dagger(\mathbf{r} - \mathbf{Q}(t)) + \eta(\mathbf{r}, t), \quad (14)$$

where  $K^\dagger(\mathbf{r}) = K(-\mathbf{r})$ .

We now decompose the field into its average part and its fluctuating part  $\phi = \langle \phi \rangle + \psi$ , these two components obey the evolution equations

$$\frac{\partial \langle \phi(\mathbf{r}) \rangle}{\partial t} = -R\Delta \langle \phi(\mathbf{r}) \rangle + hRK^\dagger(\mathbf{r} - \mathbf{Q}(t)), \quad (15)$$

$$\frac{\partial \psi(\mathbf{r})}{\partial t} = -R\Delta\psi(\mathbf{r}) + \eta(\mathbf{r}, t). \quad (16)$$

We thus see that the mean value of the field  $\phi$  depends on the position of the inclusion but the fluctuations about this mean value are independent of the inclusion. We now write the inclusion position as  $\mathbf{Q}(t) = (\mathbf{0}, vt)$  and we write the mean value of the field  $\phi$  as

$$\langle \phi(\mathbf{r}, t) \rangle = g(\mathbf{x}, z - vt, t). \quad (17)$$

In the coordinate system  $\mathbf{r} = (\mathbf{x}, z' = z - vt)$  the equation for  $g$  is

$$\frac{\partial g}{\partial t} - v \frac{\partial g}{\partial z'} = -R\Delta g + hRK^\dagger(\mathbf{r}). \quad (18)$$

The Fourier transform of  $g$  defined as

$$\tilde{g}(\mathbf{k}) = \int d\mathbf{r} g(\mathbf{r}) \exp(-i\mathbf{k} \cdot \mathbf{r}) \quad (19)$$

obeys [15]

$$\frac{\partial \tilde{g}}{\partial t} - ik_z v \tilde{g} = -\tilde{R}\tilde{\Delta}g + h\tilde{R}\tilde{K}^\dagger. \quad (20)$$

In the steady-state regime we can ignore the temporal derivative above and find

$$\tilde{g}(\mathbf{k}) = \frac{h\tilde{R}(\mathbf{k})\tilde{K}(-\mathbf{k})}{\tilde{R}(\mathbf{k})\tilde{\Delta}(\mathbf{k}) - ik_z v}. \quad (21)$$

In the coordinate system moving with the inclusion the force is given by

$$\langle f \rangle = h \frac{\partial}{\partial z'} K g|_{\mathbf{r}=0} = \frac{h}{(2\pi)^d} \int d\mathbf{k} ik_z \tilde{K}(\mathbf{k}) \tilde{g}(\mathbf{k}), \quad (22)$$

and putting eqs. (21) and (22) together then yields

$$\langle f \rangle = \frac{h^2}{(2\pi)^d} \int d\mathbf{k} \frac{ik_z \tilde{R}(\mathbf{k})\tilde{K}(\mathbf{k})\tilde{K}(-\mathbf{k})}{\tilde{R}(\mathbf{k})\tilde{\Delta}(\mathbf{k}) - ik_z v}. \quad (23)$$

For small  $v$  this gives

$$\langle f \rangle = -\lambda v, \quad (24)$$

where the coefficient of friction  $\lambda$  is given by

$$\lambda = \frac{h^2}{(2\pi)^d} \int d\mathbf{k} \frac{k_z^2 \tilde{K}(\mathbf{k})\tilde{K}(-\mathbf{k})}{\tilde{R}(\mathbf{k})\tilde{\Delta}(\mathbf{k})^2}. \quad (25)$$

In the case where the system is isotropic, that is  $\tilde{K}$ ,  $\tilde{R}$  and  $\tilde{\Delta}$  are functions of  $k = |\mathbf{k}|$ , we find

$$\lambda = \frac{h^2}{(2\pi)^d} \int d\mathbf{k} \frac{k^2 \tilde{K}(k)^2}{\tilde{R}(k)\tilde{\Delta}(k)^2}. \quad (26)$$

We can also analyze the case where the insertion is inserted at a time  $t = 0$  and see how the force evolves in time. This case is especially interesting when the corresponding steady-state quantities turn out to be divergent. Here it is convenient to work with the Laplace transform of the average force defined as  $\bar{f}(s) = \int_0^\infty dt \exp(-st)f(t)$ . Using the fact that  $f(0) = 0$ , we can solve eq. (18) by Laplace transforming to give

$$\langle \bar{f}(s) \rangle = \frac{h^2}{s(2\pi)^d} \int d\mathbf{k} \frac{ik_z \tilde{R}(\mathbf{k})\tilde{K}(\mathbf{k})\tilde{K}(-\mathbf{k})}{\tilde{R}(\mathbf{k})\tilde{\Delta}(\mathbf{k}) + s - ik_z v}. \quad (27)$$

The static result eq. (23), when it is finite, is recovered from the pole at  $s = 0$  in eq. (27). In the limit of small  $v$  we can define a time-dependent friction coefficient  $\lambda(t)$  via  $\langle f(t) \rangle = -\lambda(t)v$ . The Laplace transform of  $\lambda(t)$  is then given by

$$\bar{\lambda}(s) = \frac{h^2}{s(2\pi)^d} \int d\mathbf{k} \frac{k_z^2 \tilde{R}(\mathbf{k})\tilde{K}(\mathbf{k})\tilde{K}(-\mathbf{k})}{(\tilde{R}(\mathbf{k})\tilde{\Delta}(\mathbf{k}) + s)^2} \quad (28)$$

and when the system is isotropic this can be written as

$$\bar{\lambda}(s) = \frac{h^2}{s(2\pi)^d} \int d\mathbf{k} \frac{k^2 \tilde{R}(k)\tilde{K}^2(k)}{(\tilde{R}(k)\tilde{\Delta}(k) + s)^2}. \quad (29)$$

Finally it is interesting to ask under what conditions a force can be generated in a direction perpendicular to the direction of the insertion's uniform motion in two or more dimensions. The calculations above can be easily extended to show that the force in the direction  $x$ , say, is given by

$$\langle f_\perp \rangle = \frac{h^2}{(2\pi)^d} \int d\mathbf{k} \frac{ik_x \tilde{R}(\mathbf{k})\tilde{K}(\mathbf{k})\tilde{K}(-\mathbf{k})}{\tilde{R}(\mathbf{k})\tilde{\Delta}(\mathbf{k}) - ik_z v}. \quad (30)$$

Note that this Hall-like effect can be analyzed for the forces on vortices in superconductors, however the evaluation of the force in this magnetic context requires a subtle analysis of the time-dependent Ginzburg-Landau equations [16–18]. In our problem the interaction between the inclusions and the field is via a pure potential so the evaluation of the corresponding forces is much more straightforward. In an isotropic system it is clear that  $\langle f_\perp \rangle = 0$ . The perpendicular friction coefficient is given via  $\langle f_\perp \rangle \sim -\lambda_\perp v$  for small  $v$  as

$$\lambda_\perp = \frac{h^2}{(2\pi)^d} \int d\mathbf{k} \frac{k_x k_z \tilde{K}(\mathbf{k})\tilde{K}(-\mathbf{k})}{\tilde{R}(\mathbf{k})\tilde{\Delta}^2(\mathbf{k})}. \quad (31)$$

An interesting example of where this perpendicular friction coefficient can be non-zero is where the interaction term takes a dipolar form  $\tilde{K}(\mathbf{k}) = -i\mathbf{d} \cdot \mathbf{k}$ , while the other operators remain isotropic, in this case we find

$$\lambda_{\perp} = \frac{2h^2 d_x d_z}{(2\pi)^d} \int d\mathbf{k} \frac{k_x^2 k_z^2}{\tilde{R}(k) \tilde{\Delta}^2(k)}, \quad (32)$$

and thus see that it can be non-zero when the dipole has non-zero components in the direction of the motion and perpendicular to the motion. For a fixed dipole modulus, the magnitude of the perpendicular force is maximal when the dipole is orientated at  $45^\circ$  to the direction of the movement. We will demonstrate the existence of this rather odd perpendicular force later on in simulations of the two-dimensional Ising model.

## 2.4 Regularization of divergences in the model

The integrals appearing in eqs. (23) and (25) may diverge. To be more specific, we will focus on the friction coefficient for an isotropic system. The divergences depend on the dimension  $d$  of the system and the operators  $\Delta$ ,  $R$  and  $K$ . For small  $k$  we will take them of the form

$$\tilde{\Delta}(k) \sim k^\delta, \quad (33)$$

$$\tilde{R}(k) \sim k^\rho, \quad (34)$$

$$\tilde{K}(k) \sim k^\alpha. \quad (35)$$

We find that the integral in eq. (25) is infrared divergent when  $d < d_c$ , with  $d_c$  given by

$$d_c = 2\delta + \rho - 2\alpha - 2. \quad (36)$$

We note that  $d_c$  increases: i) as  $\delta$  increases, *i.e.* long-distance excitations cost less energy, ii)  $\rho$  decreases, *i.e.* long-distance modes relax more quickly iii) when  $\alpha$  decreases, *i.e.* when the coupling of the inclusion to the field is long range. In the case where the drag coefficient is infrared divergent, it is regularized by cutting off the  $k$  integration at an infrared cut-off  $k_{\min} = \pi/L$ , where  $L$  is the linear system size. For  $d < d_c$  we find

$$\lambda \sim L^{d_c-d}. \quad (37)$$

As should be expected the divergence of the friction coefficient also shows up in a non-analytic behavior of the average drag force at small  $v$  and one can show that

$$\langle f \rangle \sim v^{1-\frac{d_c-d}{\rho+\delta-1}}, \quad (38)$$

when  $d < d_c$ , under the conditions  $\rho + \delta > 1$  and  $(d_c - d)/(\rho + \delta - 1) < 2$ .

Finally there is another way to regularize the infrared divergence; we can measure the friction coefficient at a finite time. We expect that the friction coefficient will grow with the time as

$$\lambda(t) \sim t^\phi, \quad (39)$$

and one can compute the exponent  $\phi$  using the Laplace transform (29). Making the change of variable  $k = s^{1/(\rho+\delta)}q$ , and noting that the Laplace transform of  $t^\phi$  is proportional to  $s^{-(1+\phi)}$ , we obtain

$$\phi = \frac{d_c - d}{\rho + \delta}, \quad (40)$$

where again we assume that  $\rho + \delta > 1$ .

In general the expressions given above for the drag force can also exhibit ultraviolet divergence which must be regularized. There are two possible physical length scales which regularize the corresponding integrals:

i) The field theory has a natural cut off  $k = \pi/a_0$ , where  $a_0$  is a length scale below which the field does not fluctuate or beyond which its fluctuations are strongly suppressed. This cut off scale can be imposed by hand and taken to correspond to a molecular scale, for example the lipid size in lipid membrane bilayers, or because the Hamiltonian function  $\tilde{\Delta}$  has corrections at higher order in  $k$  than its low  $k$  form given in eq. (35).

ii) The size of the inclusion  $a$  gives a cut off  $k = \pi/a$ , for instance instead of having a point-like magnetic field inclusion where  $\tilde{K} = h$ , one can have a Gaussian-distributed field smeared over a region of size  $a$  with  $\tilde{K} = h \exp(-\frac{k^2 a^2}{2})$ . This means that the  $k$  integration is effectively cut off at  $k = \pi/a$ . For the purposes of this paper, therefore, we will take the cut off to be  $k_{\max} = \min\{\pi/a_0, \pi/a\}$ . However in most cases of interest it is usually  $a$  which is the larger of these two ultraviolet length scales.

The conclusion of this analysis is that when  $d < d_c$  the results we obtain are dominated by the long-distance properties of the theory and we see a diverging friction coefficient as  $\xi \rightarrow 0$ . However if  $d > d_c$  the friction coefficient becomes strongly dependent on the ultraviolet cut off, for instance on the size of the inclusion. This ultraviolet-dominated regime thus lacks the universality of the infrared-dominated regime and we must be careful in our choice of model and regularization to obtain physically meaningful results.

## 2.5 Force fluctuations

Here we will consider the statistical properties of the fluctuations of the force about its mean value. Depending on the system, these fluctuations may be measurable and could provide a method for determining some of the effective parameters describing the system. We define the fluctuating component of the force as

$$\delta f = f - \langle f \rangle. \quad (41)$$

This fluctuating component can be written in terms of the fluctuating component of the field  $\psi$  defined in eq. (16) and is given by

$$\delta f = h \frac{\partial}{\partial z} K \psi|_{\mathbf{r}=\mathbf{Q}(t)}. \quad (42)$$

In the steady-state regime the correlation function of the field  $\psi$  is given by

$$\begin{aligned} \langle \psi(\mathbf{r}, t) \psi(\mathbf{r}', t') \rangle &= C(\mathbf{r} - \mathbf{r}', t, t') \\ &= T \int d\mathbf{u} \Delta(\mathbf{r} - \mathbf{u}) \exp(-|t - t'| \Delta R)(\mathbf{u} - \mathbf{r}'). \end{aligned} \quad (43)$$

Using this, we find that the correlation function for the force fluctuation is given by

$$\begin{aligned} \langle \delta f(t) \delta f(t') \rangle &= \frac{Th^2}{(2\pi)^d} \int d\mathbf{k} k_z^2 \frac{\tilde{K}(\mathbf{k}) \tilde{K}(-\mathbf{k})}{\tilde{\Delta}(\mathbf{k})} \\ &\times \exp\left(-|t - t'| \tilde{\Delta}(\mathbf{k}) \tilde{R}(\mathbf{k}) + ik_z v(t - t')\right). \end{aligned} \quad (44)$$

The equal time correlation function is thus given by

$$\langle \delta f(0) \delta f(0) \rangle = \frac{Th^2}{(2\pi)^d} \int d\mathbf{k} k_z^2 \frac{\tilde{K}(\mathbf{k}) \tilde{K}(-\mathbf{k})}{\tilde{\Delta}(\mathbf{k})}. \quad (45)$$

and is independent of the velocity  $v$ . We also see that there is a fluctuation-dissipation-like relation relating the zero-velocity force fluctuations to the linear friction coefficient:

$$\int_0^\infty dt \langle \delta f(t) \delta f(0) \rangle|_{v=0} = T\lambda. \quad (46)$$

In general any measurement of a force will not be instantaneous and will depend on the temporal resolution of the experimental set up and will thus represent force averaged over a characteristic time scale  $T_m$  associated with the force measurement apparatus. We define the temporally averaged force over the time window  $T_m$  as

$$f_m = \frac{1}{T_m} \int_0^{T_m} f(t) dt, \quad (47)$$

clearly we have  $\langle f_m \rangle = \langle f \rangle$  and the variance at zero velocity  $\sigma_m^2 = \langle (f_m - \langle f \rangle)^2 \rangle|_{v=0}$  is given, for large  $T_m$ , by

$$\sigma_m^2 = \frac{2T\lambda}{T_m}. \quad (48)$$

### 3 Numerical simulations of drag in the Ising model

In this section we perform numerical simulations of drag forces on inclusions in the Ising model. This is an example of an interacting theory where the drag forces predicted in free-field theories should also occur. Our simulations in fact show that, despite their approximative nature in the context of interacting theories, our results for the free Gaussian ferromagnet account well for the phenomenology of drag observed in Ising systems. We will consider the model on a  $d$ -dimensional cubic lattice of spacing  $a_0$ , with periodic boundary conditions, and denote by  $N$  the total number of sites and spins. The Hamiltonian is given by

$$H = -J \sum_{(i,j)} S_i S_j - h \sum_i K_{i-i_0} S_i, \quad (49)$$

where  $J > 0$  is a ferromagnetic coupling between nearest-neighbour spins and where  $hK_{i-i_0}$  is the local field at site  $i$  due to the inclusion whose position is denoted by  $i_0$ . Here the vector  $K_i$  is the discrete version of the operator  $K$  of sect. 2. In what follows, in order to fully investigate the various models discussed in the paper, but to keep to a reasonable length and minimize the amount of computation time, we will restrict our study to one and two dimensions.

The system dynamics is defined in the following manner:  $N$  elementary evolutions are performed during one unit of time. An elementary evolution consists of:

- choosing a spin set (the way of choosing it depends on the dynamics and will be given below),
- computing the energy change  $\Delta H$  associated with flipping this set of spins,
- flipping the spins with probability  $p_f = 1/(1 + \exp(\Delta H/T))$  or leaving them unchanged with probability  $1 - p_f$ .

We simulate two types of dynamics:

- Non-conserved dynamics: only one spin is chosen randomly at each step; thus the total magnetization is not conserved. This choice is referred to as Glauber dynamics.
- Conserved dynamics: at each step, two spins of opposite sign are randomly chosen; the total magnetization is conserved. This is a form of Kawasaki dynamics.

The inclusion moves in the  $z$ -direction with velocity  $v$ , so  $i_{0,z}(t) = \text{int}(vt/a_0)$  (int denoting the integer part) *i.e.* it performs one step every  $a_0/v$  units of time. To measure the force in the  $z$ -direction in a given configuration of the spins system, we compute the energy  $H_+$  if the inclusion was at the position  $i_0 + \mathbf{z}$  and  $H_-$  if it was at the position  $i_0 - \mathbf{z}$ , where  $\mathbf{z}$  is the lattice link vector in the direction  $z$ . The instantaneous force is then  $f = (H_- - H_+)/2a_0$ . Explicitly

$$f(t) = \frac{1}{2a_0} \sum_i [K_{i-(i_0+\mathbf{z})} - K_{i-(i_0-\mathbf{z})}] S_i. \quad (50)$$

As we are interested in the average force, we average over all Monte Carlo (MC) time steps after first achieving a steady state in the simulation

$$\langle f \rangle = \lim_{T_{\text{MC}} \rightarrow \infty} \frac{1}{T_{\text{MC}}} \sum_{t=1}^{T_{\text{MC}}} f(t). \quad (51)$$

We will present two kinds of plots of the results of our simulations: i) the average magnetization in the rest frame of the inclusion to see how the inclusion polarizes the spins around it and how this polarization cloud is deformed by the inclusion's movement; ii) the average drag force as a function of the velocity (*i.e.*  $\langle f \rangle(v)$ ). Note that the polarization induced by the inclusion is basically a generalization of the polaron in solid-state physics; the polaron is the response of a body's polarization field due to the presence of an electron and modifies the dynamical properties of the electron [19, 20].

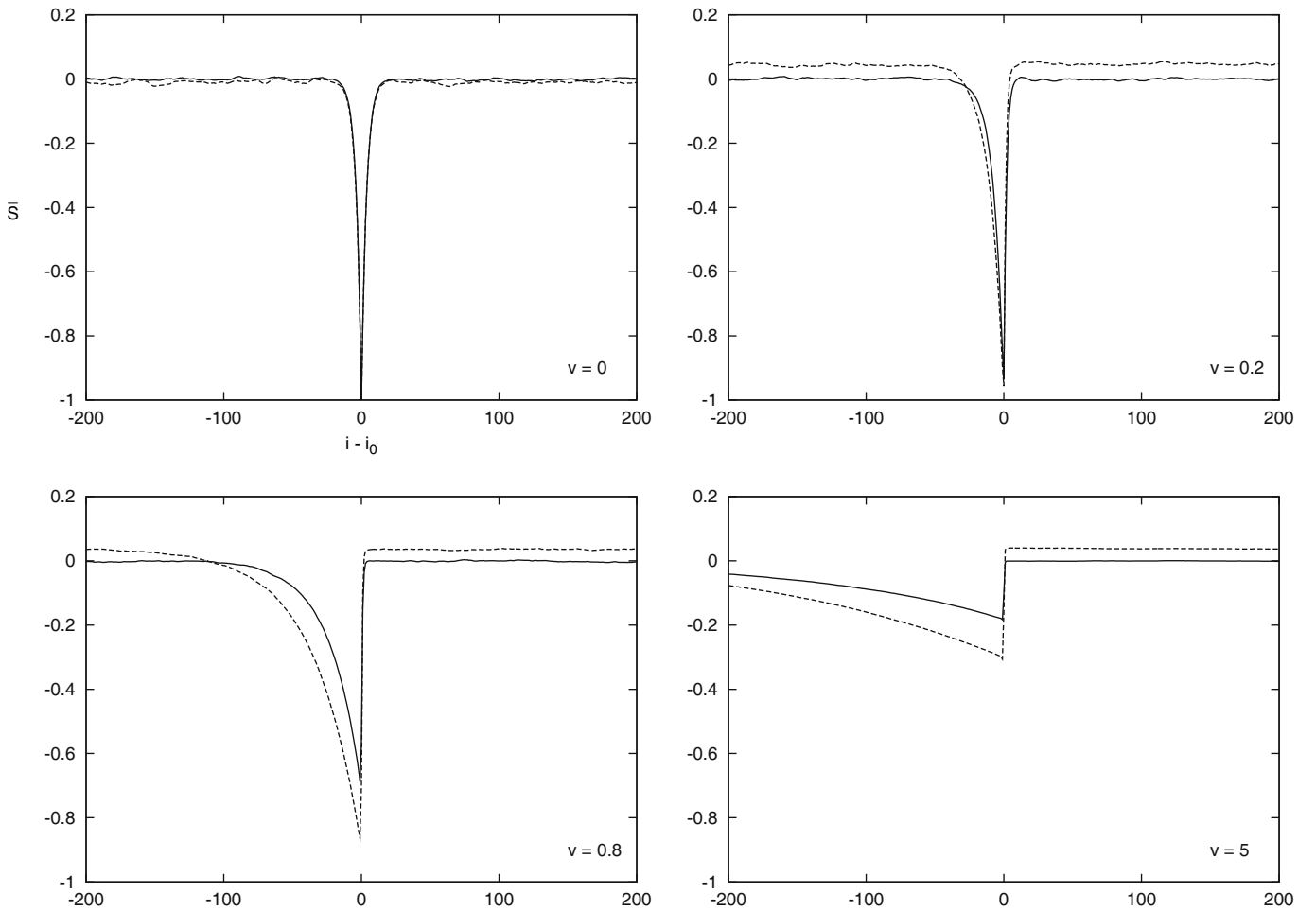


**Fig. 1.** Magnetization profile for the 1d Ising model about a local magnetic field at a single point moving with velocity  $v$ , for Glauber (solid lines) and Kawasaki (dashed lines) dynamics.

### 3.1 Point-like magnetic fields in one and two dimensions

Here we study the case where the inclusion creates a point-like magnetic field:  $K_{i-i_0} = \delta_{i,i_0}$ . We take  $h < 0$ , so that the average magnetization is (positively) proportional to the potential seen by the inclusion.

Figure 1 shows the magnetization profile for Glauber and Kawasaki dynamics, for four different speeds (with parameters  $\beta = 1$ ,  $J = 1$  and  $h = -10$ ). When the particle is at rest, it sees a spherically symmetric potential, thus it does not experience any net force. As the velocity increases, the profile becomes asymmetric and its amplitude decreases: the system has less time to react to the presence of the inclusion and thus the polaron is deformed and becomes weaker. The main differences between the two dynamics are i) the magnetization far from the particle is not zero with Kawasaki dynamics, because the total magnetization must remain zero; ii) the polaron deformation appears to be larger with Kawasaki dynamics. The mean force is plotted against the velocity in fig. 2; this figure shows that the force has a linear dependence on

$v$  for small  $v$ , reaches a maximum and then decreases as  $1/v$  for large  $v$ . The 2d simulations give similar results (figs. 3, 4). Note that in two dimensions we are in the high-temperature regime before the ferromagnetic phase transition ( $\beta = 1$ ,  $J = 0.4$ ,  $h = -6.66$ ). These behaviors are in agreement with our general results for free fields: the asymmetric profile is responsible for the force and for small  $v$  the asymmetry increases with  $v$  whereas for large  $v$  the profile amplitude diminishes. As the deformation is larger for Kawasaki dynamics, the force is larger.

The fits with our analytical results for model A and B dynamics are performed by varying three parameters: the cut-off and a dilatation for each axis of the Gaussian model to fit the Ising case. In principal the cut-off should be  $\pi$  and this is the value used in the fits for Glauber dynamics in both 1 and 2 dimensions. The fits for the cut-off in Kawasaki dynamics are 0.5 in 1d and 1 in 2d. The scaling of the  $y$  axis is due to the fact the the Gaussian model has a linear response to the field which is not the case in Ising systems (where the local magnetization can saturate). Here the scaling of the amplitudes of

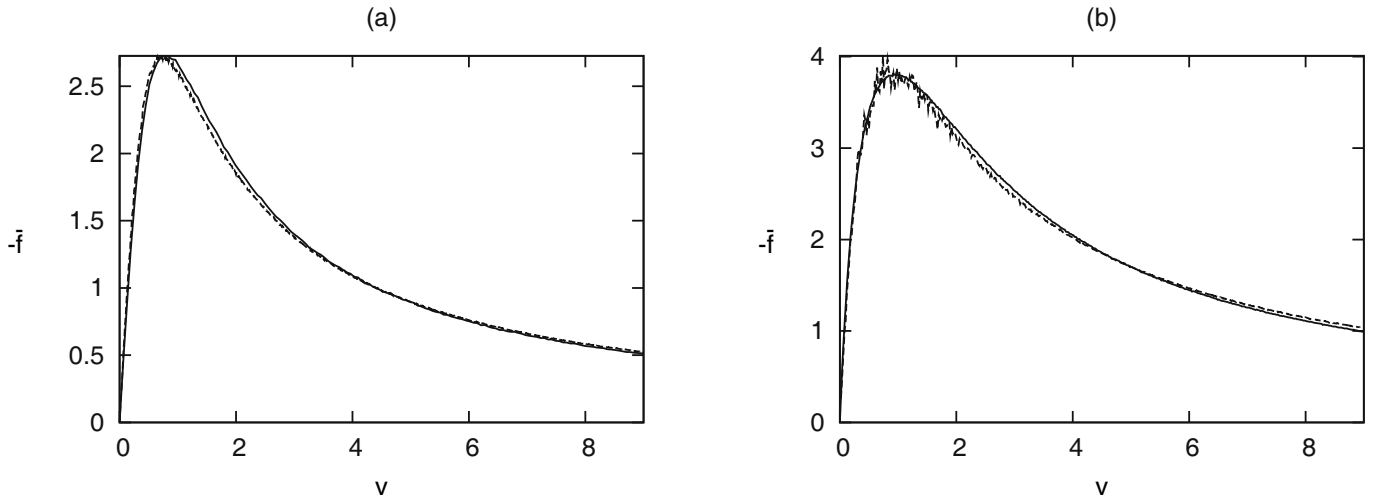


**Fig. 2.** Dashed lines: average drag force  $\bar{f}$  in the 1d Ising model as a function of  $v$  for Glauber (a) and Kawasaki dynamics (b). Solid lines are the fits of model A (a) and model B (b) dynamics for the Gaussian ferromagnet.

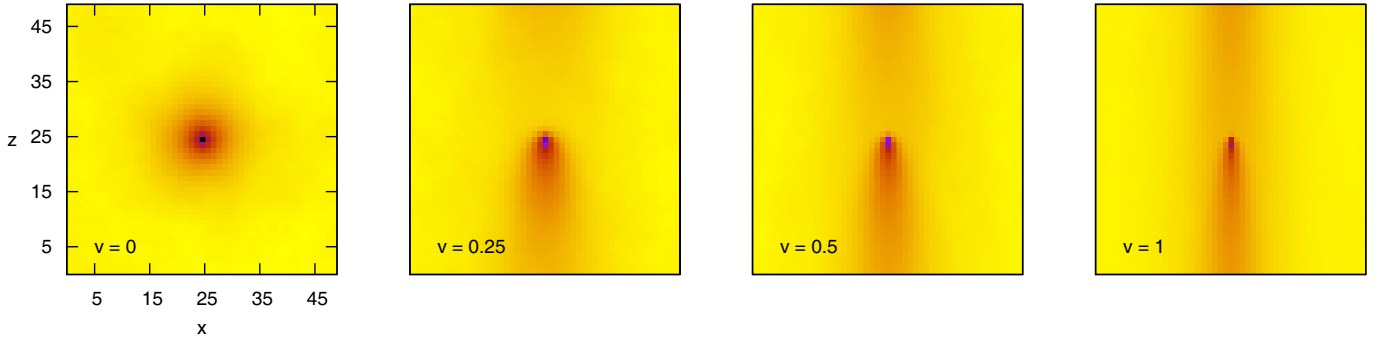


**Fig. 3.** Contour plot (color online) of the magnetization profile (polaron) for the 2d Ising model with Glauber dynamics about a local magnetic field at a single point moving with velocity  $v$ . (high temperature phase:  $\beta = 1$ ,  $J = 0.4$ ,  $h = -6.66$ ).

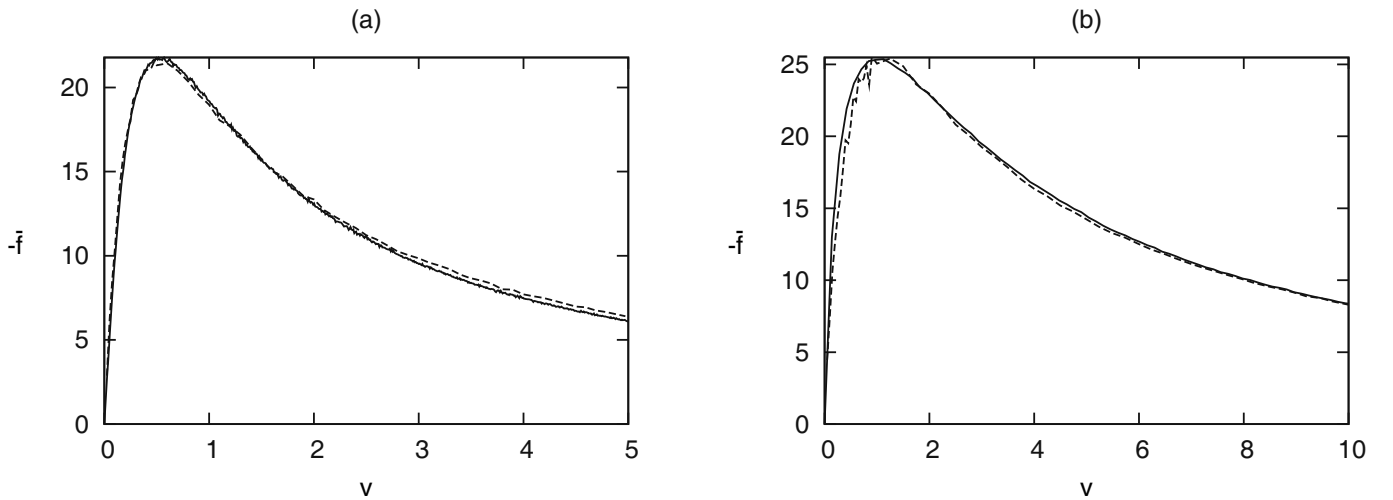


**Fig. 4.** Dashed lines: average drag force  $\bar{f}$  in the 2d Ising model as a function of  $v$  for Glauber (a) and Kawasaki dynamics (b). Solid lines are the fits of model A (a) and model B (b) dynamics for the Gaussian ferromagnet ( $\beta = 1$ ,  $J = 0.4$ ,  $h = -6.66$ ).

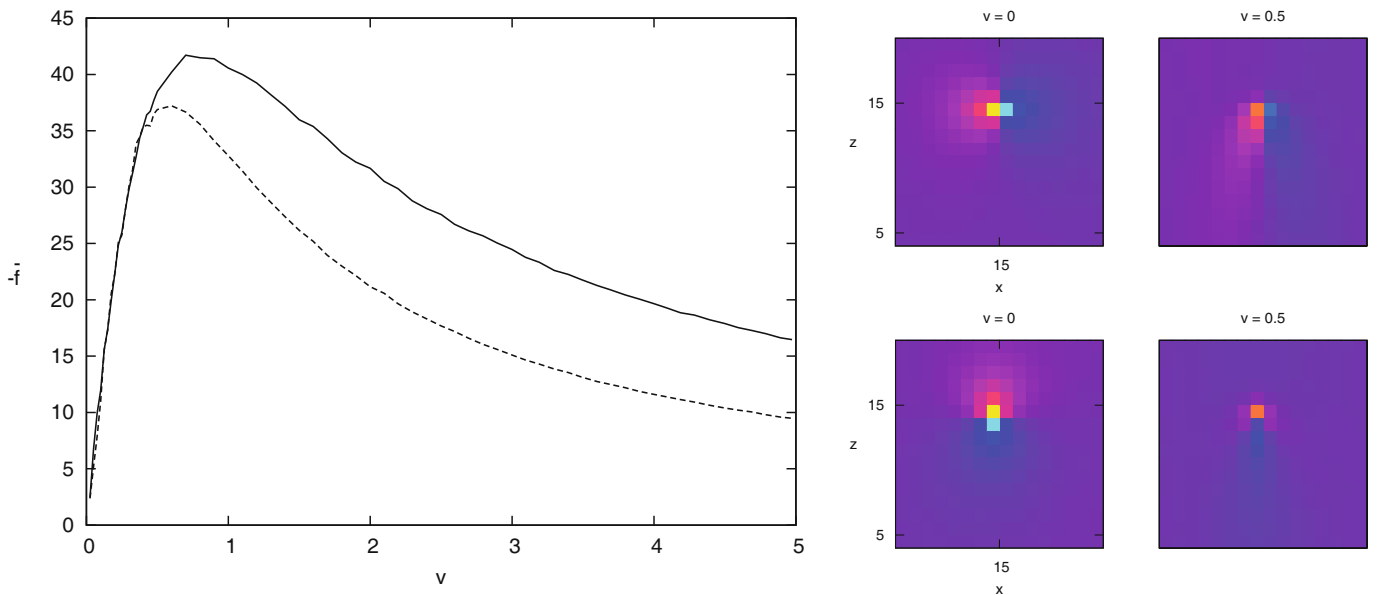


**Fig. 5.** Drag force for dipoles perpendicular (solid line) and parallel (dashed line) to the motion for Glauber dynamics ( $\beta = 1$ ,  $J = 0.4$ ,  $h = -6.66$ ). Contour plot (color online) for two values of  $v$  for dipoles perpendicular (first line) and parallel (second line) to the motion.

the drag were 2.34, 13, 5.75 and 53.5 for 1d Glauber, 1d Kawasaki, 2d Glauber and 2d Kawasaki, respectively. Finally the rescaling of the  $v$  axis corresponds to the problem of linking the time scales for the two problems and also possible differences between the correlation length in continuous and discrete models (see the discussion in sect. 4). The corresponding rescaling factors of the  $v$ 's were 0.32, 1.07, 0.17 and 0.63. These values are all order 1 and hence reasonable.

### 3.2 Dipoles in two dimensions

Here, the inclusion interacts as a dipole:  $K_{i-i_0} = (\delta_{i,i_0} - \delta_{i,i_0-\mathbf{u}})$ , where  $\mathbf{u}$  is a unit vector giving the direction of the dipole. Figure 5 shows the drag force for dipoles perpendicular ( $\mathbf{u} = \mathbf{x}$ ) and parallel ( $\mathbf{u} = \mathbf{z}$ ) to the direction of motion for Glauber dynamics. We also show the contour plots for the local magnetization profile for both cases, at velocities  $v = 0$  and  $v = 0.5$ . As seen from the force curves, at slow speed the force does not depend on the orientation, when the speed increases the force for the perpendicular dipole becomes larger.

Finally, we compare the forces parallel and perpendicular to the motion for a dipole orientated at  $45^\circ$  to the direction of the motion ( $\mathbf{u} = \mathbf{x} + \mathbf{z}$ ) in fig. 6. The force in the direction  $\mathbf{x}$  is calculated in the same way as that described above for the force in the direction  $\mathbf{z}$ . We see that the transverse force has the same order of magnitude as the longitudinal force, and the same general form. Also shown on the right is the corresponding contour plot of the local magnetization generated by the dipole at rest and for  $v = 0.5$ . Whereas at  $v = 0$  the magnetization profile appears antisymmetric about the direction of the dipole, when the dipole moves it experiences a force which pushes

it to the left on the bottom right figure of fig. 5. This is because the leading component of the dipole barely sees the polarization created by the lower component, whereas the magnetization created by the leading component pushes away the lower component.

## 4 The one-dimensional Ising model with Glauber dynamics

In sect. 2 we have analyzed the drag on inclusions in free fields. Our simulations in sect. 3 were however for the Ising ferromagnet. We showed that the force measured in these simulations could be remarkably well fitted by a free-field theory. Here we show that the drag for a point-like magnetic field in the one-dimensional Ising model with Glauber dynamics [21] can be exactly solved within the linear response regime, where  $\beta h \ll 1$ , and that the force so obtained is exactly of the form predicted from the model A dynamics for the Gaussian ferromagnet.

As in our simulations we will compute the symmetrized instantaneous force given by

$$\langle f(t) \rangle = \frac{h}{2} [\langle S_{i_0(t)+1} \rangle - \langle S_{i_0(t)-1} \rangle], \quad (52)$$

where  $i_0(t) = \text{int}(vt)$  and we have set the lattice spacing  $a_0 = 1$ . The time-dependent magnetic field in this problem can be written as

$$h_k(t) = h_0 \delta_{k, i_0(t)}. \quad (53)$$

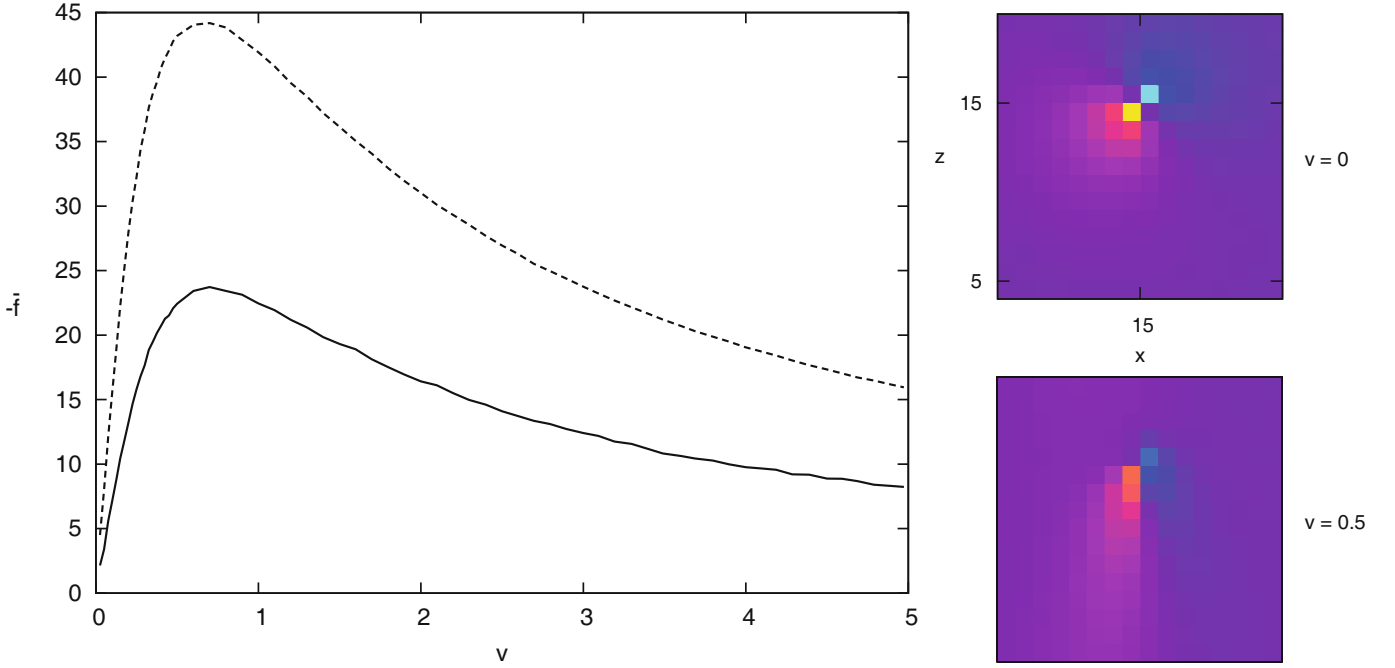


**Fig. 6.** Forces for a dipole orientated at  $45^\circ$  to the motion with Glauber dynamics. Solid line: average force perpendicular to the motion; dashed line: force parallel to the motion ( $\beta = 1$ ,  $J = 0.4$ ,  $h = -6.66$ ). Contour plot (color online) for two values of  $v$ .

We will work in the regime where the applied field is small and apply linear response theory to write

$$\langle S_j(t) \rangle = \langle S_j(t) \rangle_0 + h \sum_k \int_{-\infty}^t ds \left\langle \frac{\delta S_j(t)}{\delta h_k(s)} \right\rangle_0 \delta_{k,i_0(s)}, \quad (54)$$

where  $\langle \cdot \rangle_0$  indicates averaging in the absence of the field  $h$ . We also assume that the dynamics of the system in the absence of the field  $h$  evolves from a statistically homogeneous initial state such that

$$\langle S_i(t) \rangle_0 = \langle S_j(t) \rangle_0, \quad (55)$$

for all  $i$  and  $j$ . Along with eq. (54) in eq. (52) this yields

$$\begin{aligned} \langle f(t) \rangle &= \frac{h^2}{2} \sum_k \int_{-\infty}^t ds \left[ \left\langle \frac{\delta S_{i_0(t)+1}}{\delta h_k(s)} \right\rangle_0 - \left\langle \frac{\delta S_{i_0(t)-1}}{\delta h_k(s)} \right\rangle_0 \right] \delta_{k,i_0(t)} \\ &= \frac{h^2}{2} \int_{-\infty}^t ds \left[ \left\langle \frac{\delta S_{i_0(t)+1}}{\delta h_{i_0(s)}} \right\rangle_0 - \left\langle \frac{\delta S_{i_0(t)-1}}{\delta h_{i_0(s)}} \right\rangle_0 \right]. \end{aligned} \quad (56)$$

The response function for the unperturbed system is defined by

$$\mathcal{R}(i, j, t, s) = \left\langle \frac{\delta S_i(t)}{\delta h_j(s)} \right\rangle_0, \quad (57)$$

and for a system in thermal equilibrium we may write

$$\mathcal{R}(i, j, t, s) = \mathcal{R}(i - j, t - s), \quad (58)$$

as we have spatial and time translation invariance and thus

$$\langle f(t) \rangle = \frac{h^2}{2} \int_{-\infty}^t ds [\mathcal{R}(i_0(t) - i_0(s) + 1, t - s) - \mathcal{R}(i_0(t) - i_0(s) - 1, t - s)]. \quad (59)$$

In addition, for a system in equilibrium, one has the fluctuation dissipation theorem [22]

$$\mathcal{R}(i, j, t, s) = \beta \theta(t - s) \frac{\partial C(i, j, t, s)}{\partial s} = \beta \frac{\partial C(i - j, t - s)}{\partial s}, \quad (60)$$

for  $t > s$ , and where

$$C(i, j, t, s) = \langle S_i(t) S_j(s) \rangle_0 \quad (61)$$

is the spin-spin correlation function. Therefore at thermal equilibrium we find

$$\langle f(t) \rangle = -\frac{\beta h^2}{2} \int_{-\infty}^t ds \frac{\partial}{\partial \tau} (C(i_0(t) - i_0(s) + 1, \tau) - C(i_0(t) - i_0(s) - 1, \tau))_{\tau=t-s}. \quad (62)$$

The correlation function obeys the equation

$$\frac{\partial}{\partial t} C(i, t) = -C(i, t) + \frac{\gamma}{2} (C(i + 1, t) + C(i - 1, t)), \quad (63)$$

where  $\gamma = \tanh(2\beta J)$  [21]. We now consider a system with  $2L + 1$  spins at sites  $-L, \dots, 0, \dots, L$  and periodic boundary conditions. We define the discrete Fourier transform of  $C$  via

$$C(j) = \sum_{k=-L}^L \tilde{C}(k) \exp\left(\frac{2\pi i j k}{2L + 1}\right), \quad (64)$$

and thus the Fourier coefficients are given by

$$\tilde{C}(k) = \frac{1}{2L+1} \sum_{j=-L}^L C(j) \exp\left(-\frac{2\pi ijk}{2L+1}\right). \quad (65)$$

The initial condition for eq. (63) is given by the equilibrium correlation function

$$C(i) = \eta^{|i|}, \quad (66)$$

where  $\eta = \tanh(\beta J)$ . We can now use eq. (63) to express eq. (62) in terms of its Fourier representation to find

$$\begin{aligned} \langle f(t) \rangle &= -\beta i h^2 \int_{-\infty}^t ds \sum_k \tilde{C}(k, (t-s)) \\ &\times \left[ 1 - \gamma \cos\left(\frac{2\pi k}{2L+1}\right) \right] \\ &\times \sin\left(\frac{2\pi k}{2L+1}\right) \exp\left(\frac{2\pi i k (i_0(t) - i_0(s))}{2L+1}\right). \end{aligned} \quad (67)$$

Now in the continuum limit where  $\xi \gg 1$  we write simply that  $i_0(t) = vt$  and use the solution

$$\tilde{C}(k, t) = \tilde{C}(k, 0) \exp\left(-t \left[ 1 - \gamma \cos\left(\frac{2\pi k}{2L+1}\right) \right]\right), \quad (68)$$

to obtain

$$\langle f(t) \rangle = \beta i h^2 \sum_k \frac{\tilde{C}(k, 0) \left[ 1 - \gamma \cos\left(\frac{2\pi k}{2L+1}\right) \right] \sin\left(\frac{2\pi k}{2L+1}\right)}{1 - \gamma \cos\left(\frac{2\pi k}{2L+1}\right) - \frac{2\pi i k v}{2L+1}}. \quad (69)$$

The initial condition eq. (66) along with (65) then gives

$$\begin{aligned} \tilde{C}(k, 0) &= \frac{1}{2L+1} \sum_{j=-L}^L \eta^{|j|} \exp\left(-\frac{2\pi ijk}{2L+1}\right) \\ &= \frac{1}{2L+1} \frac{1 - \eta^2}{1 + \eta^2 - 2\eta \cos\left(\frac{2\pi k}{2L+1}\right)} \\ &= \frac{1}{2L+1} \frac{1}{\cosh(2\beta J)} \frac{1}{1 - \gamma \cos\left(\frac{2\pi k}{2L+1}\right)}, \end{aligned} \quad (70)$$

where we have taken the limit of large  $L$  and assumed that  $\eta < 1$  (*i.e.* non-zero temperature). Putting this all together then yields

$$\langle f(t) \rangle = \frac{\beta i h^2}{\cosh(2\beta J)(2L+1)} \sum_k \frac{\sin\left(\frac{2\pi k}{2L+1}\right)}{1 - \gamma \cos\left(\frac{2\pi k}{2L+1}\right) - \frac{2\pi i k v}{2L+1}}. \quad (71)$$

Now the sum can be written as an integral for  $L$  large to give

$$\langle f(t) \rangle = \frac{\beta i h^2}{2\pi \cosh(2\beta J)} \int_{-\pi}^{\pi} dk \frac{\sin(k)}{1 - \gamma \cos(k) - i k v}. \quad (72)$$

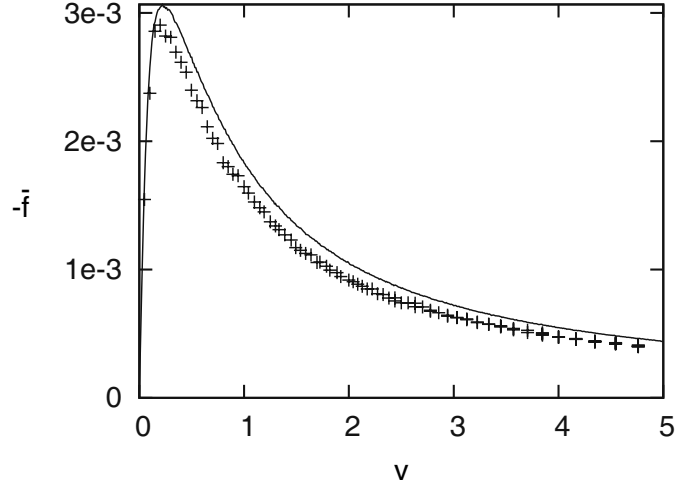


**Fig. 7.** Drag force in one dimension for small field in an Ising model with Glauber dynamics (crosses) *versus* analytical result, eq. (72) (solid line);  $\beta = 1$ ,  $J = 1.5$ ,  $h = 0.2$ .

We can recover the link with the continuum models studied here if we consider the limit where the inverse correlation length  $m \ll 1$ . Here we have

$$m = -\ln(\eta) \sim 2 \exp(-2\beta J). \quad (73)$$

If we take  $m$  small the integral in eq. (72) is dominated by its behavior at small  $k$ , in addition we have  $\gamma \sim 1 - 2 \exp(-4\beta J) = 1 - m^2/2$ , which yields

$$\langle f(t) \rangle = \frac{\beta i m h^2}{\pi} \int_{-\pi}^{\pi} dk, \frac{k}{k^2 + m^2 - 2i k v}, \quad (74)$$

which has the same form as that for model A dynamics for a Gaussian ferromagnet.

The analytical result (72) has been compared with a simulation; the results given fig. 7 show a good agreement between them. We interpret the fact that the analytical result overestimates the simulations result as a trace of a nonlinear response in the field  $h$ .

## 5 Application to proteins in lipid membrane

### 5.1 General analysis

Here we will try and investigate some possible sources of drag in lipid membrane models. A way of estimating the diffusion constant of an insertion, such as a protein in a lipid membrane, is via the Stokes Einstein relation

$$D = \frac{k_B T}{\lambda_t}, \quad (75)$$

where  $\lambda_t$  is the total friction on the protein. The Stokes-Einstein relation is in fact only rigorously valid for a friction coefficient computed from the *average* velocity at *fixed* force, *i.e.* via

$$f = \lambda \langle v \rangle. \quad (76)$$

However, when the average value of the force is large compared to its fluctuations, we should be in a limit where the Stokes-Einstein relation using a friction coefficient computed in the constant velocity ensemble gives a good estimate. Hence if the coupling to the membrane  $h$  is large, the resulting average force will be large,  $O(h^2)$  with respect to the force fluctuations which are, from eq. (45)  $O(h)$ . However for this statement to be valid one needs to be in a system where the linear-response regime is wide enough such that the force still behaves as  $\lambda v$ , even when it is bigger than its fluctuations. This will clearly always become the case for  $h$  sufficiently large. Of course, there will be in general many other sources of drag in the problem (other fields, hydrodynamic effects, etc.). Thus the results we present are valid in the case where i) the average force in the range of  $v$  where linear response applies is bigger than the fluctuations of the force and ii) the drag created by the field we are considering dominates over all other drags. The range of validity of the results is thus severely constrained. In what follows we do not claim to explain the experimental literature on membrane inclusion diffusion constants but rather try to show what types of behavior could be generated for certain types of interaction fields, their couplings to inclusion position and their dynamics. Finally we should also mention that height fluctuations of the membrane even when they are not coupled to the position insertion can lead to an apparent slowing down of diffusion [23] as the projected area of the membrane is smaller than its physical area (within which the protein diffuses), this means that the projection of the diffusion will appear to be slowed down, we will not consider this effect in what follows.

There are also many possible sources of drag which should be taken into account, however when the drag force computed here is large compared to the other drag forces we can safely ignore the others. There are a number of possible sources of drag in lipid membranes. The first treatment of this problem was by Saffmann and Delbrück (SD) [11] who computed the hydrodynamic drag by treating the low Reynolds number Navier Stokes equations for a slab of flat 2d fluid containing a solid cylindrical insertion. The movement of the fluid sets up a hydrodynamic flow and the resulting friction on the cylinder is computed using the stress tensor. The coupling to the bulk external fluid is very important and is essential to find a finite result for the drag, as a purely two-dimensional treatment gives a divergent result coming from the long-range nature of hydrodynamic interactions in two dimensions. The hydrodynamic drag computed by SD is given by

$$\lambda_{\text{hydro}} = \frac{4\pi\eta_m}{\left[\ln\left(\frac{\eta_m h}{\eta_w a}\right) - \gamma\right]}, \quad (77)$$

where  $a$  is the cylinder radius and  $\eta_m$  and  $\eta_w$  are the viscosities of the membrane and surrounding fluids, respectively. The term  $h$  represents the height of the cylinder or membrane and  $\gamma \approx 0.5772$  is Euler's constant. This formula is valid in the regime where  $a \gg h$ , *i.e.* for proteins which are large relative to the membrane thickness and when  $\eta_m \gg \eta_w$ . The coupling of the 2d flow to the 3d fluid

is very important in this hydrodynamic treatment, for example if there is a hard wall in the proximity of the fluid membrane, the behavior of the diffusion constant changes to  $D \sim 1/a^2$  [24,25].

Recently in [26] a detailed experimental study, and comparison of other results in the literature, of protein diffusion constants seems to suggest that for membrane proteins and peptides the diffusion constant scales as  $D \sim 1/a$  (which is consequently a much stronger dependence on the protein radius than  $D \sim \ln(1/a)$  predicted by SD). In [26] it is suggested that the apparent failure of the SD formula may be due to the fact that the membrane is quite heterogeneous on small length scales and that the model of a perfect incompressible fluid is perhaps not well adapted for small inclusions. It is also pointed out that on larger length scales thermal fluctuations and undulations may dissipate velocity gradients. Indeed extensive numerical simulations have shown that the coupling of the protein position to local membrane curvature (and hence height fluctuations) reduces the diffusion constant of inclusions [27] and scaling arguments show that proteins whose hydrophobic cores are mismatched with the equilibrium thickness of the lipid bilayer also experience additional drag forces [28]. The effect of mismatch is clearly seen in some of the experimental studies reported in [26].

In the spirit of the comments of [26] and the study of [28], we will tentatively examine various scenarios leading to drag forces on membrane inclusions which are linearly coupled to physical fields in the membrane. We should bear in mind the limitations of this approach. First it is clear that we are ignoring possible hydrodynamic flows created by the movement of the inclusion. If substantial hydrodynamics flows are established by protein movement, then the order parameter field  $\phi$  (depending on its precise nature) can be expected to be convected with the flow. Clearly this effect is ignored in our study, however for small inclusions where the inclusion pushes past the local lipids, rather than entraining a hydrodynamic flow, we expect this approximation to be good, at least concerning orders of magnitude estimates. Secondly there is also a nonlinear coupling between inclusion position and the fluctuating field (due to the absence of the field in the region of the inclusion). However if the linear coupling is sufficiently strong, the contribution of the mean-field-like term we compute here should dominate the drag due to nonlinear terms.

In  $d = 2$ , the friction coefficient (26) reads

$$\lambda = \frac{h^2}{2\pi} \int_0^{\pi/a_c} dk, \frac{k^3 \tilde{K}^2(k)}{\tilde{R}(k) \tilde{\Delta}^2(k)}, \quad (78)$$

where  $a_c$  is the short-distance cut-off scale corresponding to the larger of the two scales  $a$ , the insertion size, and  $a_0$ , the underlying cut-off for the field fluctuations. In our models, the operators will be of the forms of eqs. (33)–(35). Here we give general expressions for the operator  $\Delta$ , the composed operator  $R\Delta$  and the coupling operator  $K$ . In order to be more precise, we write them in the dimen-

sionful form (in terms of their Fourier transforms):

$$\tilde{\Delta}(k) = \mu_{\Delta} a_0^{\delta'} k^{\delta'} (k^2 + m^2), \quad (79)$$

$$\tilde{R}(k) \tilde{\Delta}(k) = \tau_0^{-1} a_0^{\rho+\delta'+2} k^{\rho+\delta'} (k^2 + m^2), \quad (80)$$

$$\tilde{K}(k) = \mu_K a_0^{\alpha} k^{\alpha}, \quad (81)$$

where  $\mu_{\Delta}$  and  $\mu_K$  are energies and  $\tau_0$  is a microscopic time scale associated with the dynamics. The notation here is slightly different from the previous sections, where the term  $m$  strictly denoted a mass defined by  $m^2 = \tilde{\Delta}(0)$ , and also corresponds to the inverse correlation length of the field  $m = 1/\xi$ . In the Helfrich Hamiltonian, we can write  $\tilde{\Delta} \sim k^2(k^2 + m^2)$  where  $m^2 = \sigma/\kappa$ . Though  $m$  is not a mass, in this case it still corresponds to the inverse correlation length, we thus persist with the notation  $m$ .

Using these expressions in the integral above, we obtain for the friction coefficient

$$\lambda = \frac{\tau_0 \mu_K^2}{2\pi \mu_{\Delta} a_0^2} h^2 (ma_0)^{2\alpha-\rho-2\delta'} g_{\lambda} \left( \frac{ma_c}{\pi} \right), \quad (82)$$

where the function  $g_{\lambda}$  is defined by

$$g_{\lambda}(x) = \int_0^{\frac{1}{x}} dq \frac{q^{3+2\alpha-\rho-2\delta'}}{(q^2+1)^2}. \quad (83)$$

In the following, we assume that this integral is not infrared divergent, *i.e.* that  $2\delta' + \rho - 2\alpha < 4$ ; this reads  $d = 2 > d_c$  with the critical dimension (36).

It now remains to determine how the amplitude of the interaction  $h$  should be computed. It is clear that the value of  $h$  should depend on the value of the size of the inclusion. A simple, semi-macroscopic, way of doing this, proposed in [10], is the following. The energy of interaction between the field  $\phi$  and the inclusion is easily computed from the free field theory and is given by

$$\epsilon = -\frac{h^2}{2(2\pi)} \int_0^{\frac{\pi}{a_c}} dk \frac{k \tilde{K}^2(k)}{\tilde{\Delta}(k)}. \quad (84)$$

We now expect that  $\epsilon$  is a function of  $a$  and that for small  $a$

$$\epsilon(a) \sim -2\pi\gamma_I a - \pi\sigma_I a^2, \quad (85)$$

where  $\gamma_I$  and  $\sigma_I$  are effective (negative) line and surface tensions for the inclusion in the membrane due to the interaction with the field  $\phi$ . Now if we assume that  $a$  is small, in the sense that we can neglect the surface tension term, equating eq. (84) and eq. (85), we find

$$2\pi\gamma_I a = \frac{h^2}{2(2\pi)} \frac{\mu_K^2 (a_0 m)^{2\alpha-\delta'}}{\mu_{\Delta}} g_{\epsilon} \left( \frac{ma_c}{\pi} \right), \quad (86)$$

where

$$g_{\epsilon}(x) = \int_0^{\frac{1}{x}} dq \frac{q^{2\alpha-\delta'+1}}{q^2+1}. \quad (87)$$

Using the resulting expression for  $h$  in terms of  $\gamma_I$  and  $a$ , we then obtain

$$\lambda = \frac{4\pi\gamma_I a \tau_0 g_{\lambda} \left( \frac{ma_c}{\pi} \right)}{a_0^2 (ma_0)^{\rho+\delta'} g_{\epsilon} \left( \frac{ma_c}{\pi} \right)}. \quad (88)$$

Before examining a number of models of proteins inserted into membranes, we will explore a few general consequences of the above expression. Given that we expect  $a$  and  $a_0$  to be small, we should consider the functions  $g_{\lambda}$  and  $g_{\epsilon}$  in the limit  $x \rightarrow 0$ . The integrals defining these functions are finite (and thus independent of  $a$ ) in the cases where  $2\alpha - \rho - 2\delta' < 0$  and  $2\alpha - \delta' < 0$ , respectively. In this case we find the generic behavior

$$\lambda \approx \frac{4\pi\gamma_I a \tau_0 g_{\lambda}(0)}{a_0^2 (ma_0)^{\rho+\delta'} g_{\epsilon}(0)}. \quad (89)$$

In this scenario we see that the dependence of the friction coefficient on the inclusion size is always linear and it has a strong dependence on the correlation length of the field  $\phi$ . The scaling of the friction coefficient with the inclusion size is  $\lambda \sim a$ , if this drag dominates all other sources of drag application of the Stokes-Einstein relation gives

$$D \sim \frac{1}{a}. \quad (90)$$

Note that we will also recover this dependence on  $a$  if it is the case that  $a < a_0$ , *i.e.* the underlying cut-off of the field  $\phi$  is greater than the one corresponding to the inclusion size. Note that, apart from the hydrodynamic case where  $\rho = -1$ ,  $\rho$  is positive or zero, therefore if  $2\alpha - \delta' < 0$ , then  $2\alpha - \rho - 2\delta' < 0$  also. In the case where  $2\alpha - \rho - 2\delta' > 0$  and which in most cases will also imply that  $2\alpha - \delta' > 0$ , the integrals defining both  $g_{\lambda}(x)$  and  $g_{\epsilon}(x)$  will diverge and we find

$$g_{\lambda}(x) \sim \frac{1}{2\alpha - \rho - 2\delta'} \frac{1}{x^{2\alpha-\rho-2\delta'}}, \quad (91)$$

$$g_{\epsilon}(x) \sim \frac{1}{2\alpha - \delta'} \frac{1}{x^{2\alpha-\delta'}}, \quad (92)$$

and thus

$$\lambda \approx \frac{4\pi\gamma_I a \tau_0}{a_0^2} \frac{2\alpha - \delta'}{2\alpha - \rho - 2\delta'} \left( \frac{a}{\pi a_0} \right)^{\rho+\delta'}. \quad (93)$$

Again if this drag dominates, it gives a diffusion coefficient scaling with inclusion size as

$$D \sim \frac{1}{a^{\rho+\delta'+1}}. \quad (94)$$

In this case we see a different dependence on the inclusion size  $a$ , the physics of the problem is controlled by short-distance behavior and the drag is independent of the correlation length  $\xi = 1/m$  of the fluctuating field. A final possible case is where  $2\alpha - \rho - 2\delta' < 0$ , but  $2\alpha - \delta' > 0$ , in which case we find

$$\lambda \approx \frac{4\pi\gamma_I a \tau_0 g_{\lambda}(0) (ma)^{2\alpha-\delta'}}{a_0^2 (ma_0)^{\rho+\delta'} \pi^{2\alpha-\delta'}}, \quad (95)$$

this is a particularly interesting case as the friction coefficient has a strong dependence on both the correlation length of the field  $\phi$  and on the inclusion size. Again if this drag dominates the diffusion constant scaling with inclusion size is

$$D \sim \frac{1}{a^{2\alpha+1-\delta'}}. \quad (96)$$

We now discuss some specific models.

### 5.2 Insertion with curvature coupled to membrane height fluctuations

In [27] the authors numerically investigated the diffusion constant of inclusions in model membrane systems where the inclusion tends to impose a preferred local curvature on the membrane. In their model a quadratic coupling was also considered. Here we consider the model with a simple linear coupling. The inclusion is coupled to the membrane height fluctuations, the Gaussian Hamiltonian of which  $\Delta$  is given by eq. (7), the dynamical operator  $R$  is given by eq. (13) and  $K$  by eq. (10). After Fourier transforming, we obtain  $\tilde{\Delta}(k) = \kappa k^2(k^2 + m^2)$  (with  $m = \sqrt{\sigma/\kappa}$ ),  $\tilde{R}(k) = (4\eta k)^{-1}$  and  $\tilde{K}(k) = -k^2$ . In our general notation we have  $\delta' = 2$ ,  $\alpha = 2$  and  $\rho = -1$  and we are in the case where  $2\alpha - \delta' = 2$  and  $2\alpha - \rho - 2\delta' = 1$ . In terms of the physical parameters of this model the drag coefficient for small insertion size  $a$  is thus given by

$$\lambda = \frac{32\eta\gamma_I a^2}{\kappa}, \quad (97)$$

and the dominance of this drag would imply that

$$D \sim \frac{1}{a^2}. \quad (98)$$

We thus see that this result is quite insensitive to the correlation length of the height fluctuations (and thus the surface tension) assuming that they are large with respect to the insertion size.

### 5.3 Insertion coupled to a non-conserved order parameter

An insertion such as a protein or peptide can couple to various physical fields in a lipid membrane other than the height fluctuations. For instance in a lipid monolayer local tilt angles of the lipid heads or tails may be changed by the presence of an inclusion. Also if there are several lipid phases such as liquid gel and solid, the inclusion may prefer to be in one of these phases. This general idea can be modelled by assuming that the inclusion couples linearly to the order parameter representing one of these fields. The simplest Hamiltonian for this order parameter has the form of that for the Gaussian ferromagnet where  $\tilde{\Delta}(k) \propto k^2 + m^2$ . The simplest diffusive dynamics is given by model A dynamics with  $\tilde{R}(k) \propto 1$  and a linear coupling to the field  $\phi$  gives  $\tilde{K}(k) = 1$ . This dynamical model does not conserve the integrated field as there is no reason that it should be conserved. Here, in our general notation, we have  $\delta' = 0$ ,  $\alpha = 0$  and  $\rho = 0$  and we are thus in the case where  $2\alpha - \delta' = 0$  and  $2\alpha - \rho - 2\delta' = 0$ . We see that we are in the marginal case for both functions  $g_\lambda$  and  $g_\epsilon$ . Furthermore we can identify the time scale  $\tau_0$  using the diffusion constant for the dynamics of the field  $\phi$ ,  $D_0$ ,

via  $D_0\tau_0 = a_0^2$ , where  $a_0$  is the lipid size and  $D_0$  can be estimated from the lipid translational diffusion constant or lipid rotational diffusion constant, depending on the field in question (for instance if the field in question describes the orientational order of the lipids, then the lipid rotational diffusion constant could be used to give the appropriate time scale). Here for small  $x$  we find

$$g_\lambda(x) \approx -\ln(x) \quad \text{and} \quad g_\epsilon(x) \approx -\ln(x), \quad (99)$$

which leads to

$$\lambda \approx \frac{4\pi\gamma_I a}{D_0}, \quad (100)$$

and gives an estimation of the insertion diffusion constant:

$$D \approx \frac{k_B T D_0}{4\pi\gamma_I a}. \quad (101)$$

### 5.4 Insertion coupled to a conserved order parameter

The insertion may also be coupled to a conserved field, describing, for example, the local lipid composition in the case where there are several lipid types. We take the same  $\Delta$  and  $K$  operator to describe the energy of the order parameter describing local chemical composition. However we now use a conserved dynamics:  $R$  is set by (12), giving  $\tilde{R}(k) \propto k^2$ . We thus have  $\delta' = 0$ ,  $\alpha = 0$  and  $\rho = 2$ , which gives  $2\alpha - \delta' = 0$  and  $2\alpha - \rho - 2\delta' = -2$ . The function  $g_\epsilon$  is unchanged but we find  $g_\lambda \approx 1/2$  which gives

$$\lambda = \frac{2\pi\gamma_I a}{D_0 a_0^2 m^2 \ln\left(\frac{\pi}{ma}\right)}, \quad (102)$$

where we have again used  $D_0\tau_0 = a_0^2$ , and where  $D_0$  can be estimated from the lipid translational diffusion constant. This leads to the estimate

$$D = \frac{k_B T D_0 a_0^2 m^2 \ln\left(\frac{\pi}{ma}\right)}{2\pi\gamma_I a} \quad (103)$$

for the protein diffusion constant. We should note that even though there is a logarithmic correction, we would expect to experimentally measure  $D \sim 1/a$ , as the logarithmic term would require decades of length scales (thus leaving the realm of validity of the calculation) to detect. Interestingly here, in contrast with the previous models, we should see a strong dependence of  $D$  on the correlation length of the field.

## 6 Conclusions

We have seen that inclusions which are linearly coupled to classical fields with dissipative dynamics are subject to drag forces which exhibit a rather rich behavior. Notably, the drag force is a non-monotonic function of the inclusion velocity  $v$ . Generically the force is a linear function of the velocity at small  $v$  and is characterized by a friction coefficient  $\lambda$ . The force then attains a maximum value, and

for large  $v$  decays as  $1/v$ . The force is physically generated by the deformation of the polarization profile of the field about the inclusion by the inclusions motion. This phenomenon is analogous to the way in which electron dynamics is renormalized by their associated polaron in solid-state physics [19,20]. The linear coefficient of friction  $\lambda$  is of particular importance as it can be used to estimate diffusion constants via the Stokes-Einstein relation and because it can exhibit divergent behavior when the corresponding field theory is critical, *i.e.* has a diverging correlation length, for example at a critical demixing transition.

The results we have presented are valid for free or Gaussian field theories. We were able to compute the drag for the one-dimensional Ising model for a weak inclusion-field interaction but it would be interesting to go beyond the Gaussian approximation to understand the physics of drag forces for general interacting field theories. Having said this, we note that the Gaussian model does seem to capture most of the phenomenology seen in our simulations of the one- and two-dimensional Ising model.

Finally the experimental measurement of these drag forces presents an interesting challenge. It may be possible to carry out experiments using atomic force microscopy or magnetic force microscopy if the interaction between the microscopic tip and the surface can be sufficiently well characterized. Also, the thermal or critical Casimir force predicted by Fisher and de Gennes [29] has recently been successfully measured [30] in a binary fluid mixture at criticality. It may be that the technical advances made to carry out this measurement, the chemical treatment to tune the interaction between the fluid components and surfaces, and the optical force measurements could be applied to the study of the drag problem. We note also that, beyond measurements of the average force, it would also be interesting if the predictions made here about force fluctuations could be verified experimentally.

DSD thanks the Institut Universitaire de France for financial support. We would also like to thank S. Ramaswamy for helpful comments and pointing out a number of useful references.

## References

1. S. Weinberg, *The Quantum Theory of Fields*, Vol. 1 (Cambridge University Press, Cambridge, 2005).
2. M. Goulian, R. Bruinsma, P. Pincus, *Europhys. Lett.* **22**, 145 (1993).
3. E. Sackmann, in *Structure and Dynamics of Membranes, From Cells to Vesicles*, edited by R. Lipowsky, E. Sackmann (Elsevier Science BV, Amsterdam, 1995).
4. H. Imura, K. Okano, *Phys. Lett. A* **42**, 403 (1973).
5. G. Ryskin, M. Kremenetsky, *Phys. Rev. Lett.* **67**, 1574 (1991).
6. E. Dubois-Violette, E. Guazzelli, J. Prost, *Philos. Mag. A* **48**, 727 (1983).
7. T.C. Lubensky, S. Ramaswamy, J. Toner, *Phys. Rev. B* **33**, 7715 (1986).
8. C. Fusco, D.E. Wolf, U. Nowak, *Phys. Rev. B* **77**, 174426 (2008).
9. M.P. Magiera, L. Brendel, D.E. Wolf, U. Nowak, *EPL* **87**, 26002 (2009).
10. V. Démery, D.S. Dean, *Phys. Rev. Lett.* **104**, 080601 (2010).
11. P.G. Saffmann, M. Delbrück, *Proc. Natl. Acad. Sci. U.S.A.* **72**, 3111 (1975).
12. D.S. Dean, A. Gopinathan, *J. Stat. Mech.* L08001 (2009).
13. W. Helfrich, *Z. Naturforsch.* **28c**, 693 (1973).
14. P.M. Chaikin, T.C. Lubensky, *Principles of Condensed Matter Physics* (Cambridge University Press, Cambridge, 2000).
15. Solving the problem in Fourier space ensures that derivatives so computed are averaged over their left and right values (Dirichlet's theorem), this thus corresponds to our method of computing the force via the difference in energy of a move forwards and a move backwards.
16. L.P. Gor'kov, N.B. Kopnin, *Sov. Phys. Usp.* **18**, 496 (1975).
17. A.T. Dorsey, *Phys. Rev. B* **46**, 8376 (1992).
18. R.A. Simha, S. Ramaswamy, *Phys. Rev. Lett.* **83**, 3285 (1999).
19. L.D. Landau, *Phys. Z. Sowjetunion* **3**, 644 (1933).
20. H. Fröhlich, *Adv. Phys.* **3**, 325 (1954).
21. R.J. Glauber, *J. Math. Phys.* **4**, 294 (1963).
22. E. Lippiello, F. Corberi, M. Zannetti, *Phys. Rev. E* **71**, 036104 (2005).
23. A. Naji, F.L.H. Brown, *J. Chem. Phys.* **126**, 235103 (2007).
24. E. Evans, E. Sackmann, *J. Fluid Mech.* **194**, 553 (1988).
25. R. Merkel, E. Sackmann, E. Evans, *J. Phys. (Paris)* **50**, 1535 (1989).
26. Y. Gambin *et al.*, *Proc. Natl. Acad. Sci. U.S.A.* **103**, 2089 (2006).
27. A. Naji, P.J. Atzberger, F.L.H. Brown, *Phys. Rev. Lett.* **102**, 138102 (2009).
28. A. Naji, A.J. Levine, P.A. Pincus, *Biophys. J.* **93**, L49 (2007).
29. M.E. Fisher, P.-G. de Gennes, *C. R. Acad. Sci. Paris, Ser. B* **287**, 207 (1978).
30. C. Hertlein, L. Helden, A. Gambassi, S. Dietrich, C. Bechinger, *Nature* **451**, 172 (2008).